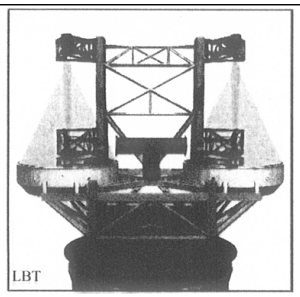

6. Types of interferometers

- MTF of a real interferometer
- The Fizeau recombination
- The classical Michelson recombination
- Other methods to carry the radiation phase
  - single-mode optical fibers
  - heterodyning the radiation
- Delay lines, coherencing or cophasing
- Field-of-view of an interferometer
- Polarisation effects
- The *densified pupil* Michelson recombination

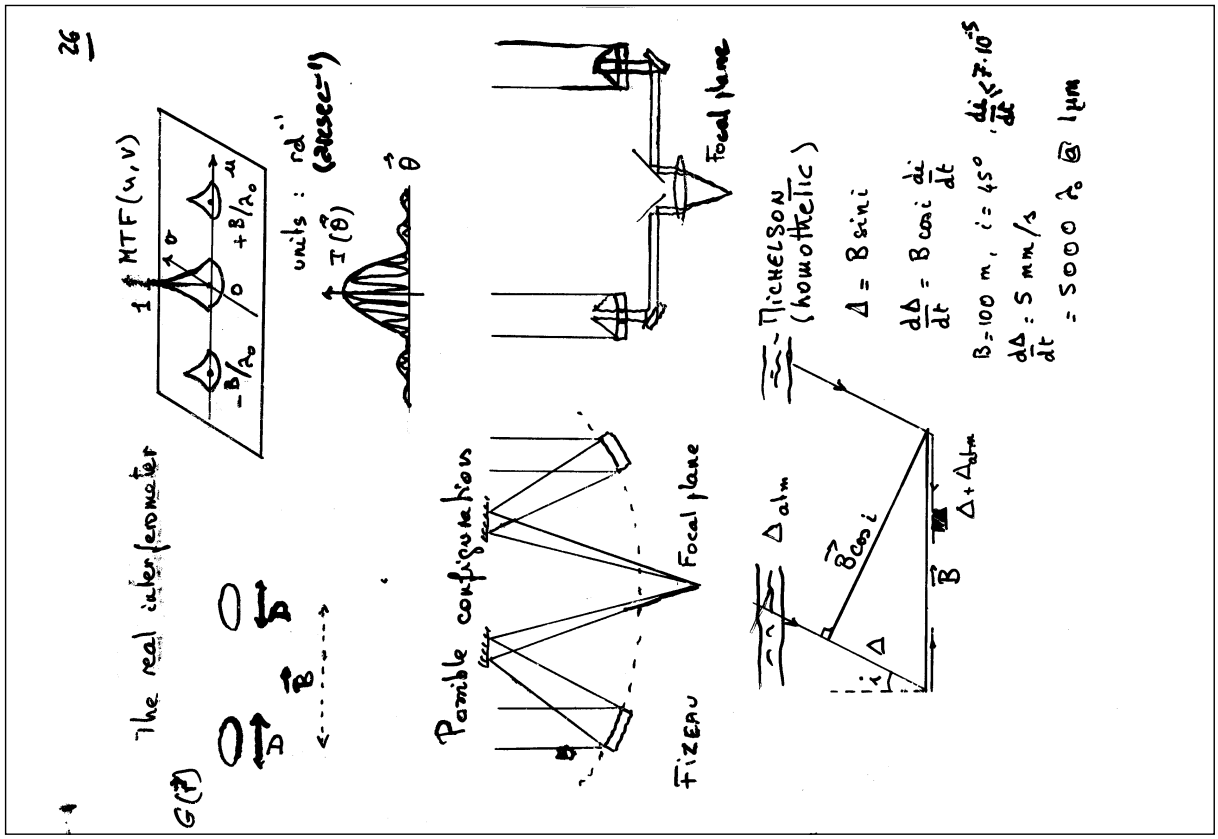

Fibres optiques

- ouverture numérique : $\sin\theta = \left(n^2_{coeur} - n^2_{gaine}\right)^{1/2}$

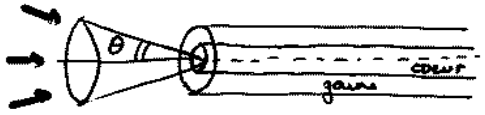

- atténuation

  db/km : $-10 \log \frac{I_{out}}{I_{in}}$

- longueur d'onde de coupure (monomode) λ_c

  $\lambda < \lambda_c$ propagé

  $\lambda > \lambda_c$ non-propagé

- efficacité de couplage

- polarisation

Schema de l'interferometre FLUOR

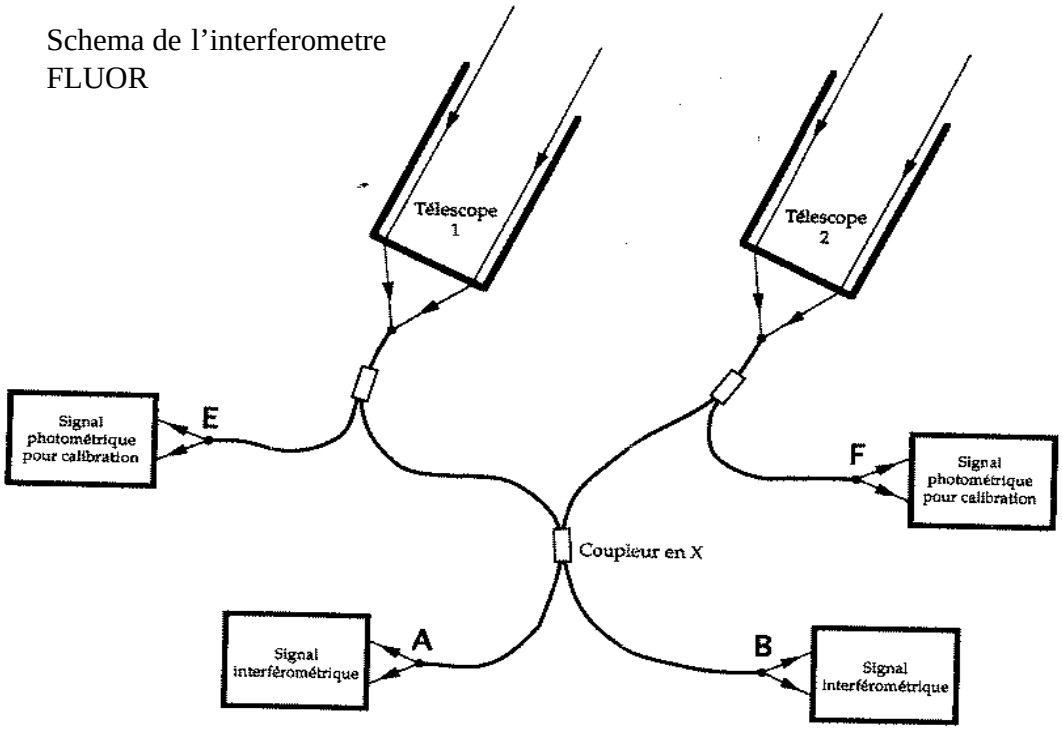

Coude du Foresto, Ridgway,Mariotti

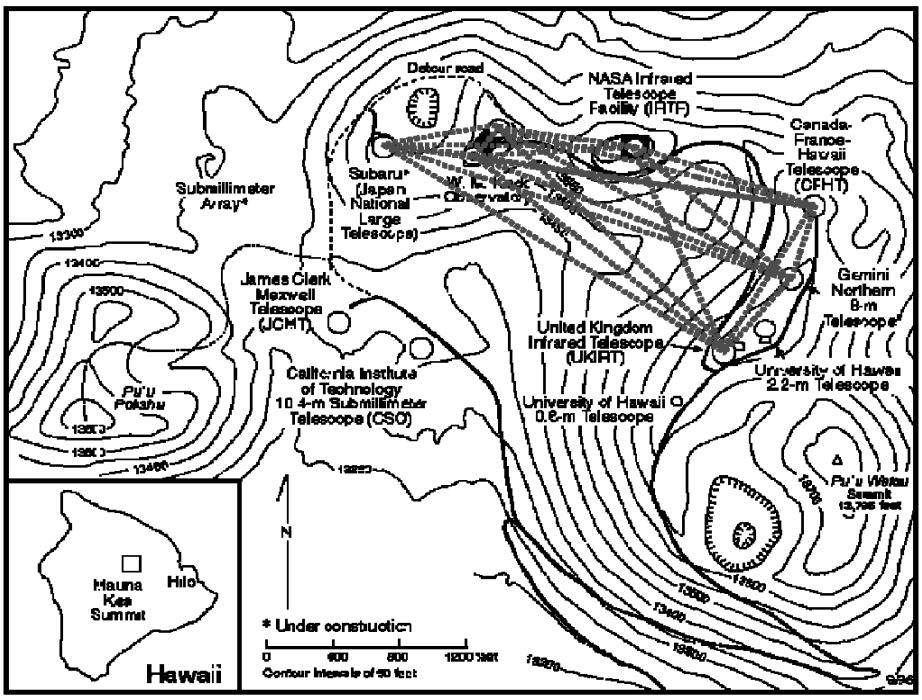

D=400m : λ/D = 2 mas @ 4μm
λ/D = 20 mas @ 40μm

From J. M. Mariotti et al. : Interferometric connection of large ground-based telescopes

3 telescope beam combiners: 2 examples under development

Coaxial scheme:

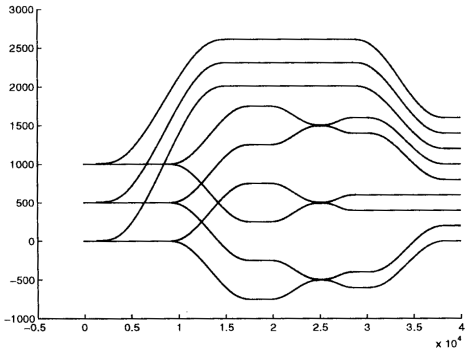

Multiaxial scheme:

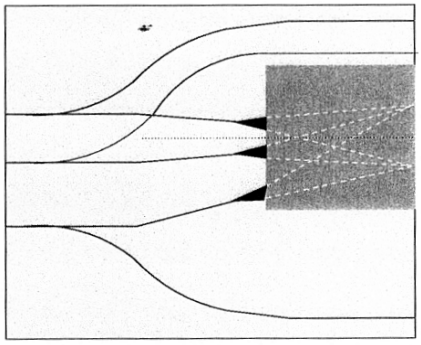

Main characteristics:

- Temporal encoding of fringes (coaxial combination).
- Pairwise beam combination.

(Severi et al, Torino,1999)

Main characteristics:

- Spatial encoding of fringes.
- Alltogether beam combination.

SFO - Bordeaux - 7 septembre 1999

Optique intégrée : fonctions de recombinaison d'un interféromètre

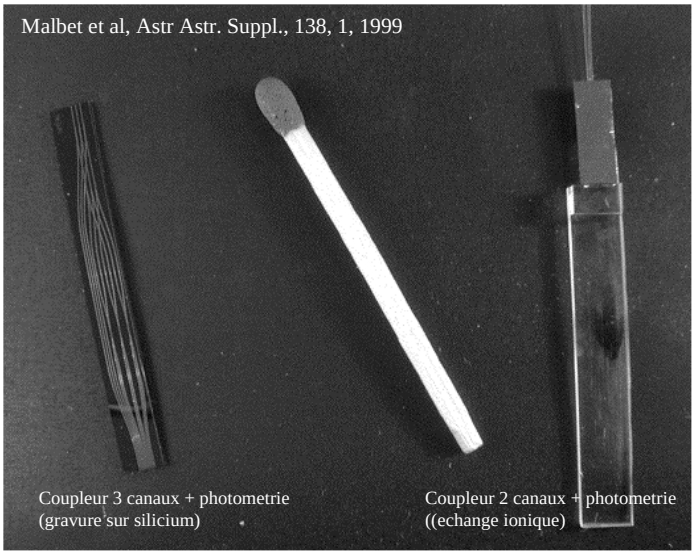

J-Ph. Berger, These, Universite Joseph Fourier, 199 (LAOG)

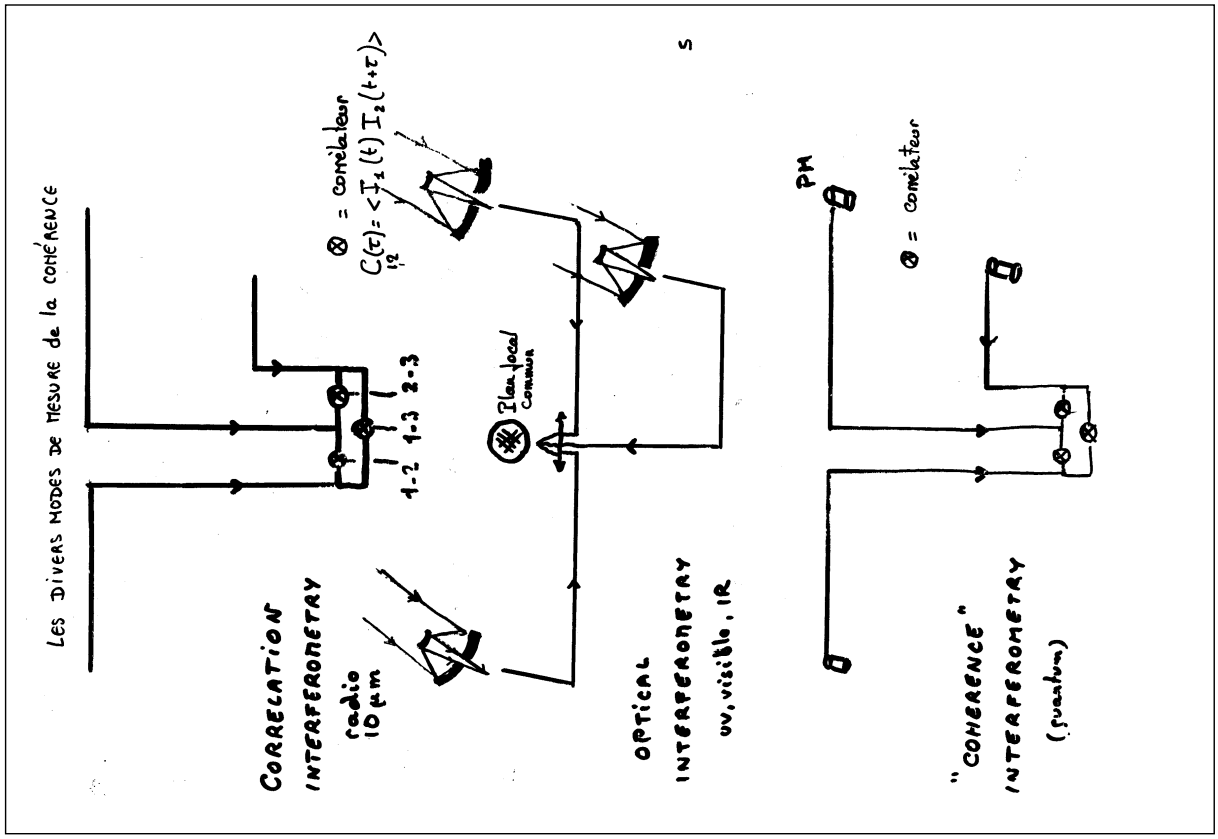

The VLTI Delay Line

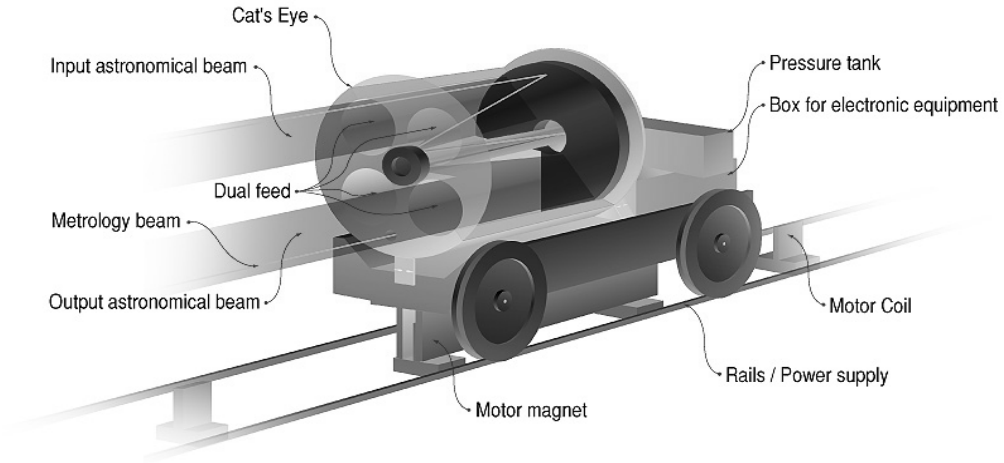

Retroreflector (Ritchey-Chretien type, "cat's eye")
mounted on a moving carriage.

- OPD range: > 120 meters
- OPD resolution: < 20 nm
- Maximum velocity: 0.5 m/sec
- Velocity accuracy:1 um/sec
- Field of view: 200 arcsec

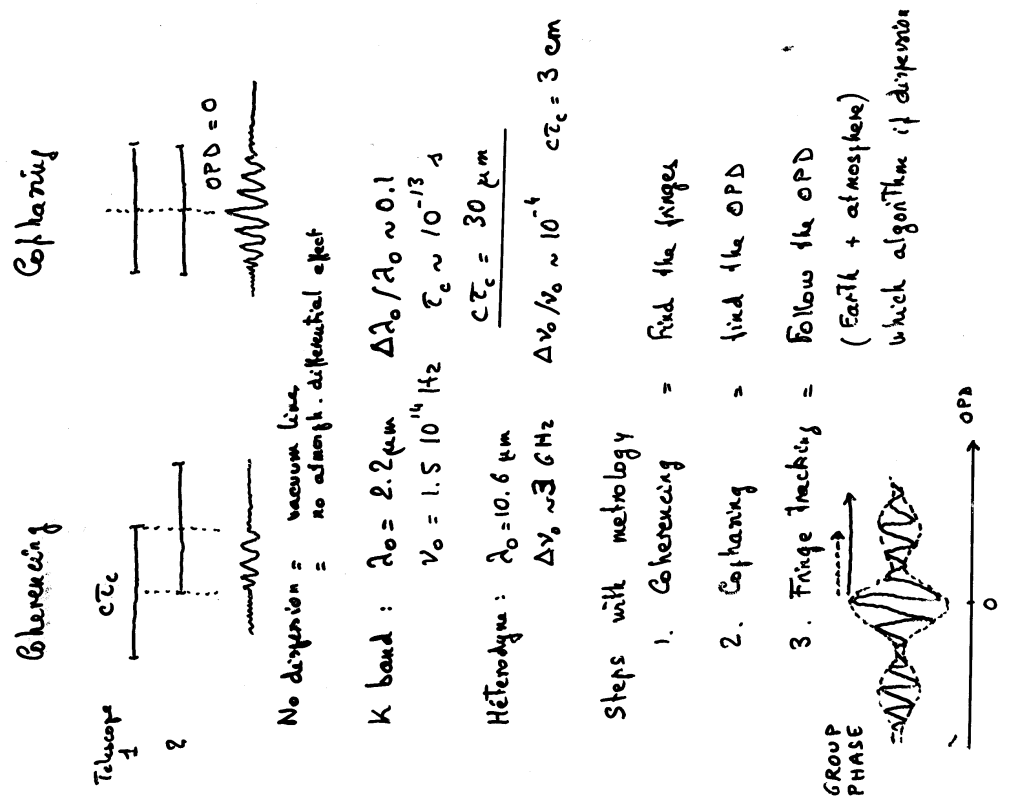

6.3

Field of view

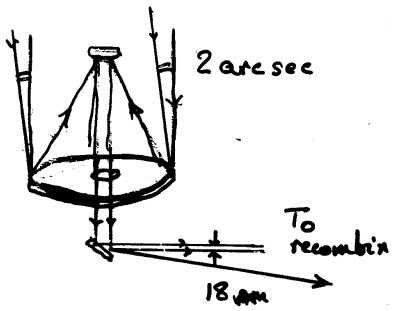

$2'' = 10^{-5}$ rd

$10^{-5} \times \frac{8}{0.18} \sim 4.10^{-4}$ rd

over 100 m ⇒ 4 cm

Field of view is a serious concern in optical interferometry

Polarization

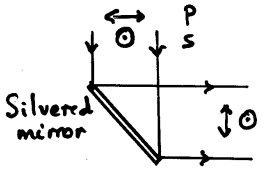

loss :

$V_{pol} = \cos\left|\frac{\varphi_S - \varphi_P}{2}\right|$

$\Delta\varphi_{sp} \sim 30°$ at 500 nm (λ^{-1})

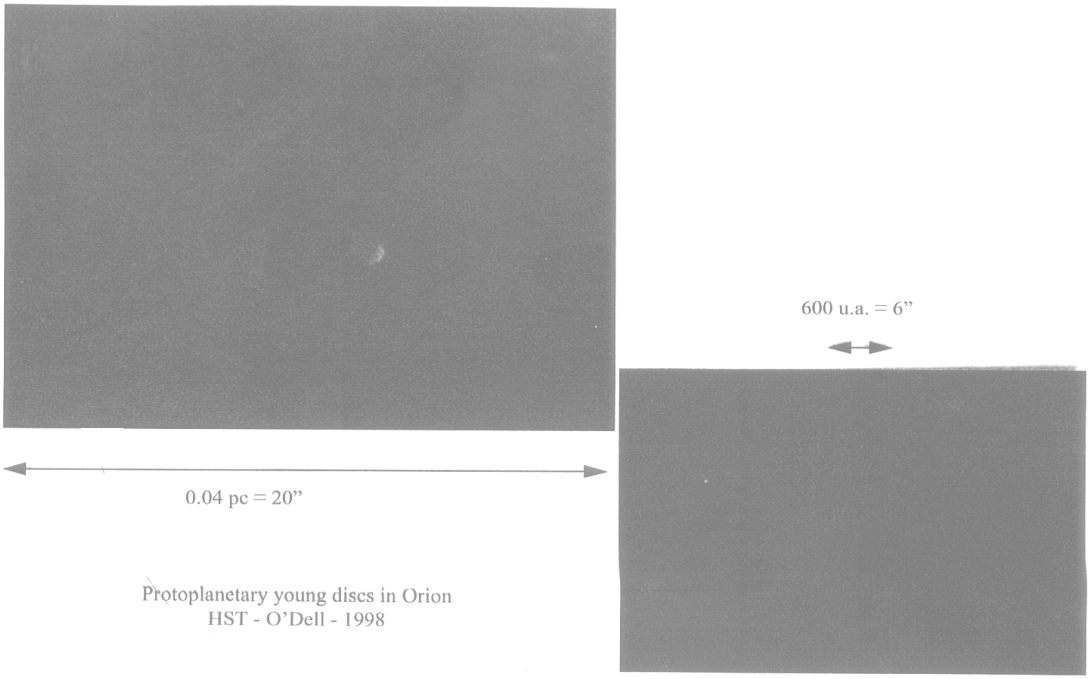

Protoplanetary young discs in Orion
HST - O'Dell - 1998

SFO - 1999 - Bordeaux

Détection directe (1) : photocentre étoile-planète

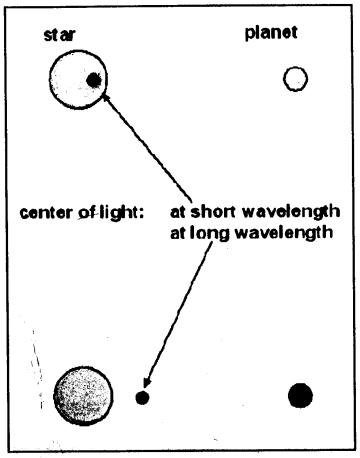

1.5 µm

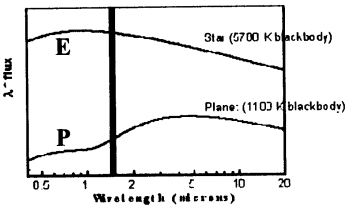

Spectres de l'étoile et de la planète

5 µm

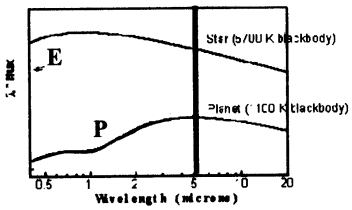

Mesure interférométrique différentielle du déplacement du photocentre étoile-planète à deux longueurs d'onde

Source : The Keck Interferometer, Science Requirements Document, Rév. 2.2, May 98, G. van Belle & G. Vashist

- "Jupiters" chauds (1300-600 K) à λ = 1.6-10 µm
- distance 0.15 au de l'étoile, éloignée de < 10 pc
- magnitudeK < 10 : 1000 étoiles cibles
- résolution spectrale 100 : CH_4, H_2O, NH_3
- précision différentielle : **10^{-3} radians**

SFO - Bordeaux - 1999

Imagerie par densification de pupille (5)
(Labeyrie 1996)

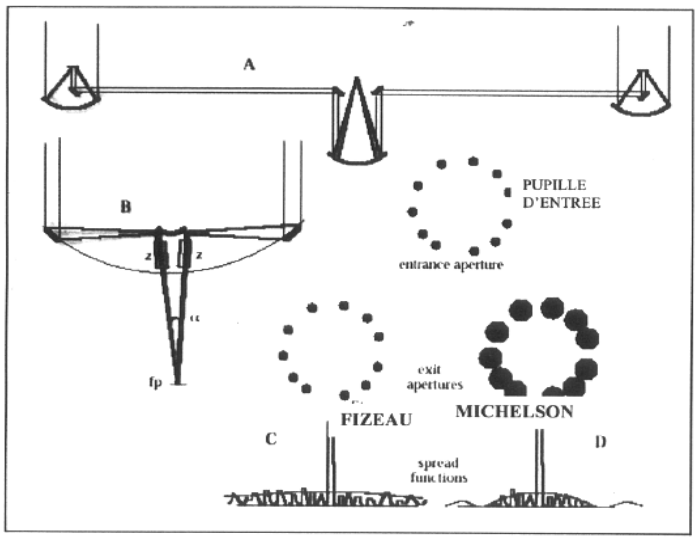

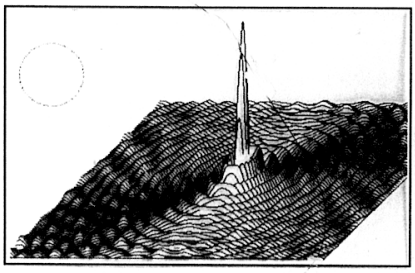

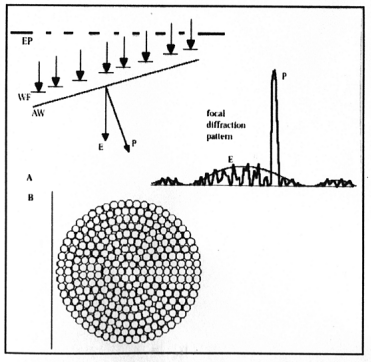

Astr.Astr.Suppl.Ser., **118**, 517, 1996

7. Effects of the Earth'a atmosphere

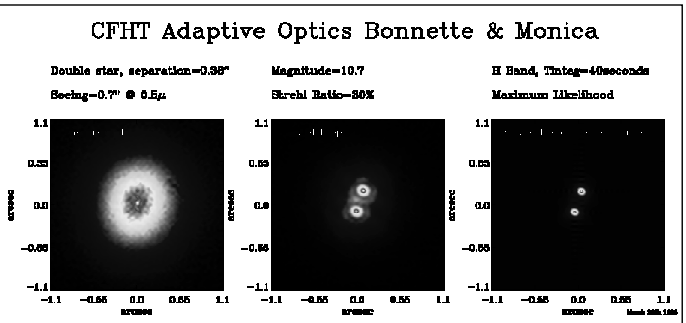

- **Overview on atmospheric coherence loss**
- **Parameters : r0(λ),** τ0(λ), θ0(λ), **L0, l0**
- **Adaptive optics, principle**

– **Zernike polynomials description of wavefront**
– **Strehl ratio S**

- **Effects on interferometric observables**

– **speckled fringes and visibility degradation**
– **piston noise**

- **Fringe dispersion & group delay**

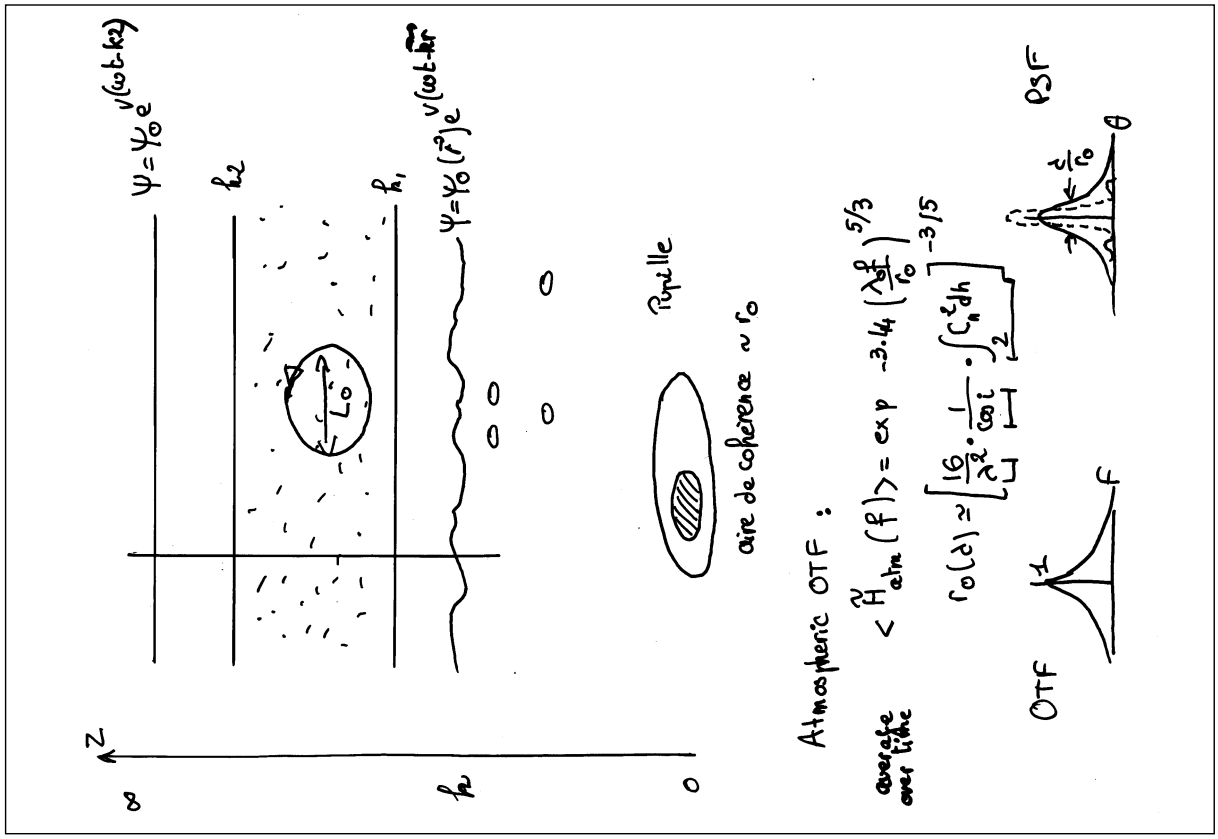

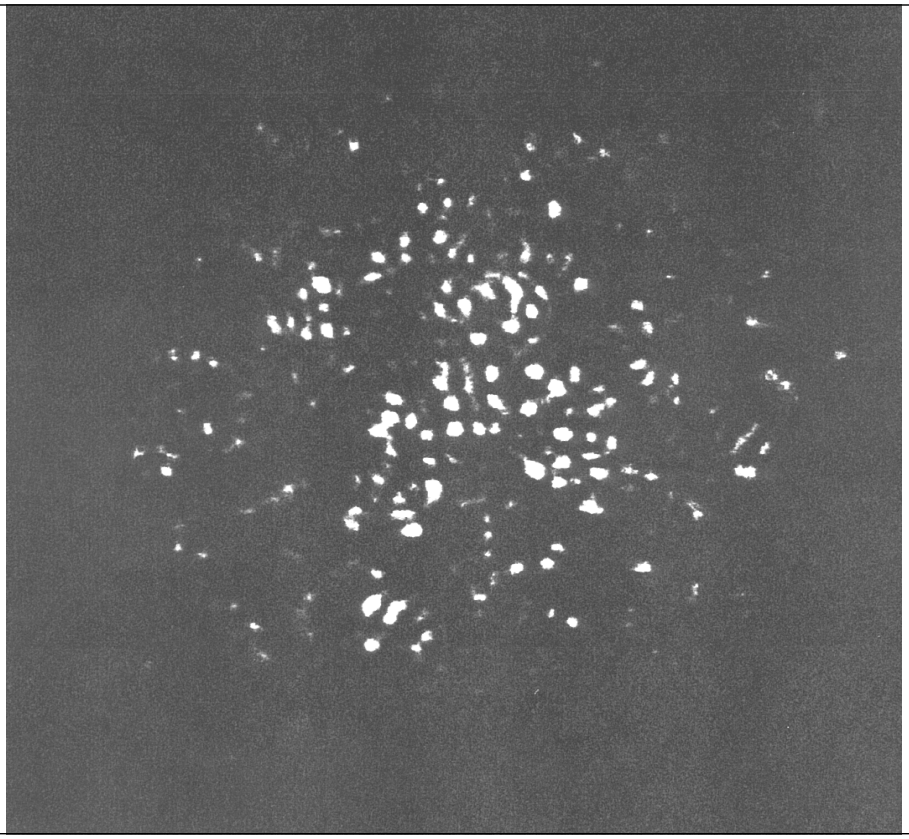

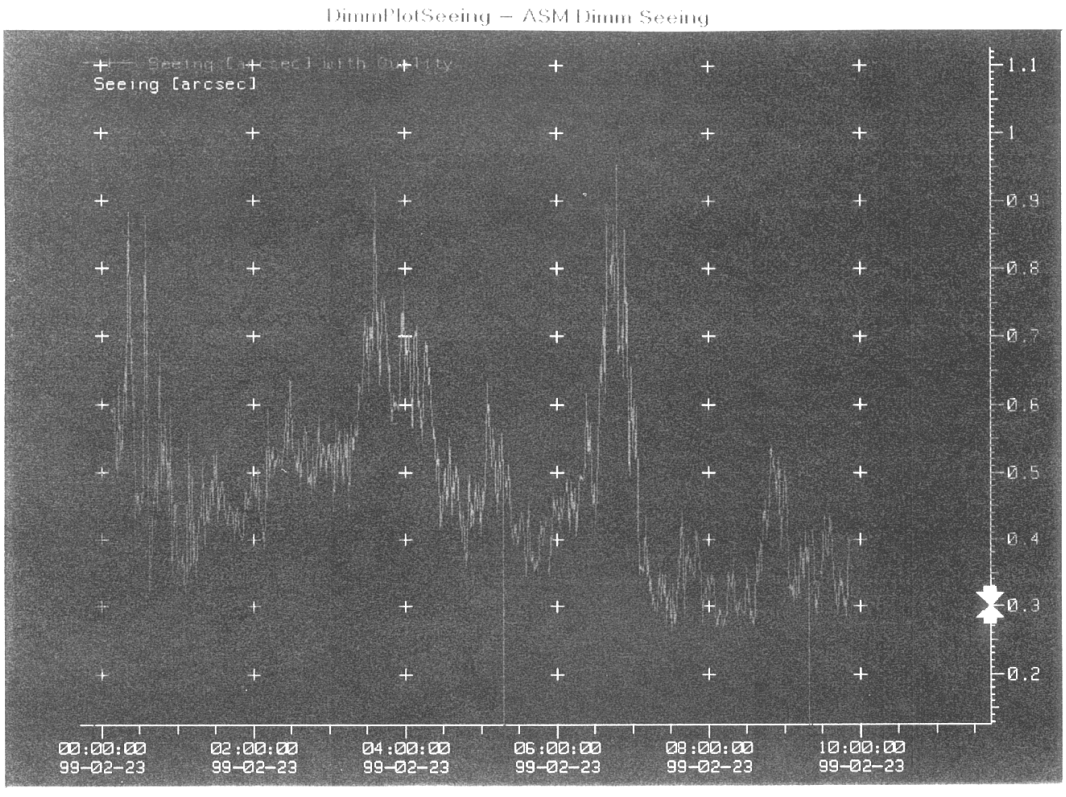
DimmPlotSeeing – ASM Dimm Seeing
Seeing [arcsec]
1.1
1
0.9
0.8
0.7
0.6
0.5
0.4
0.3
0.2
00:00:00 99-02-23
02:00:00 99-02-23
04:00:00 99-02-23
06:00:00 99-02-23
08:00:00 99-02-23
10:00:00 99-02-23

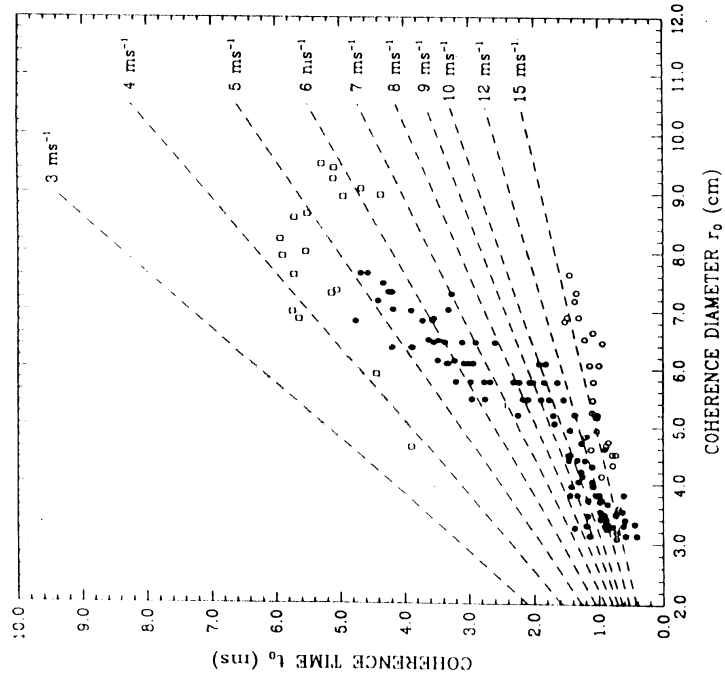

$$t_0 = 0.314\frac{r_0}{V}$$

where V is the "average windspeed" carrying the turbulent layers past the interferometer.

Chatterton Astronomy Department

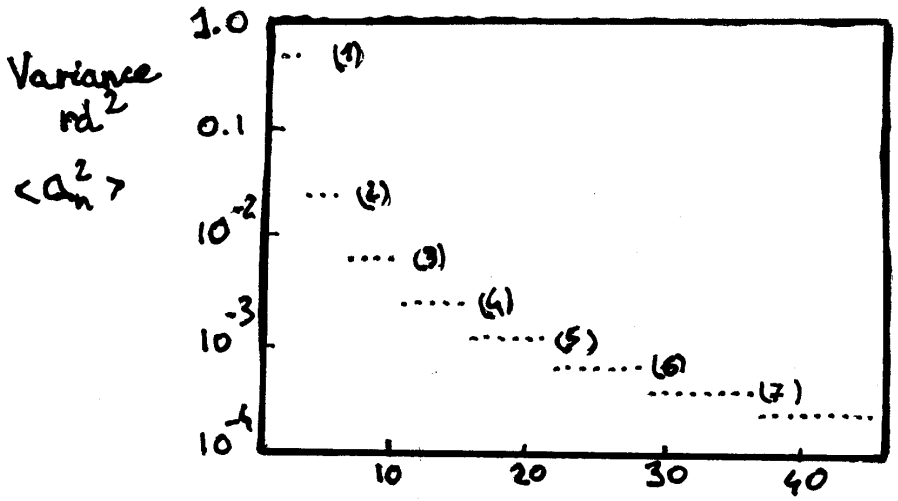

$L_0 = \infty$, donc indépendant du diamètre D

Si $L_0 \downarrow$, $\langle a_n^2 \rangle \downarrow$

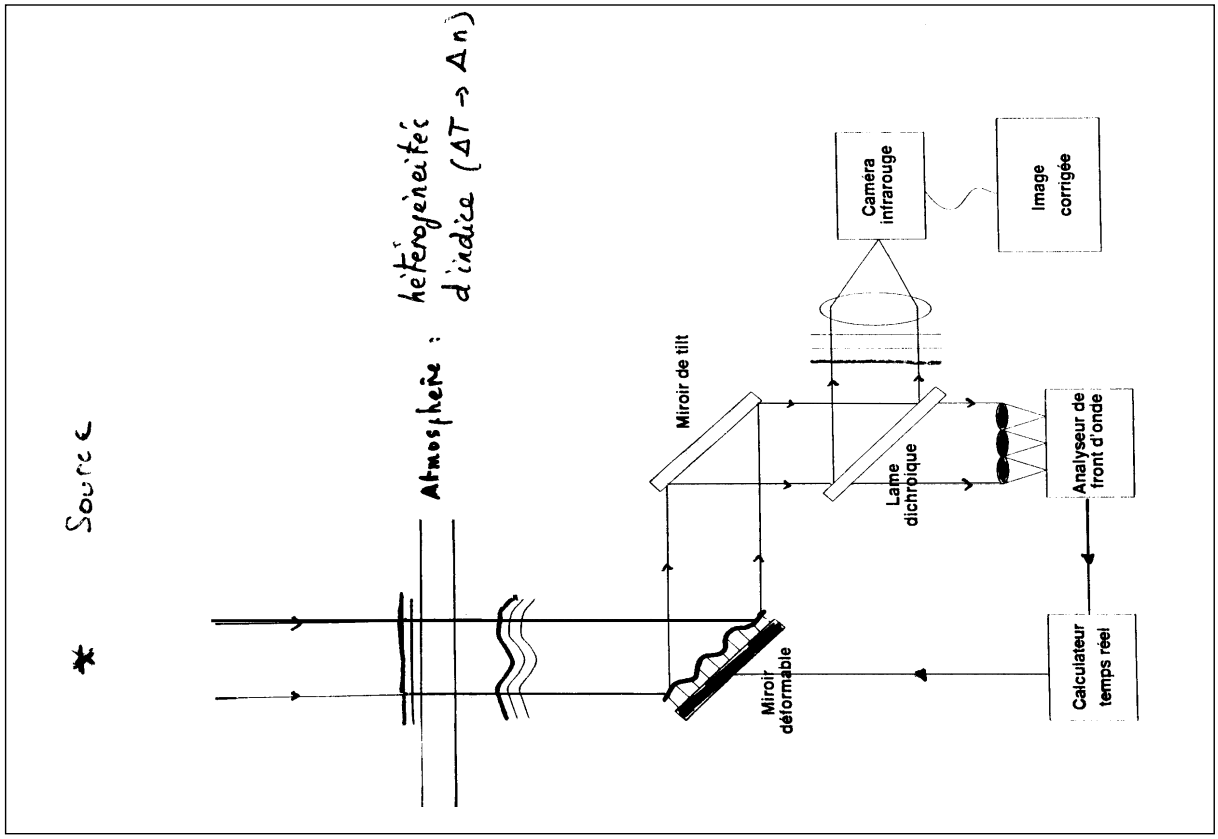

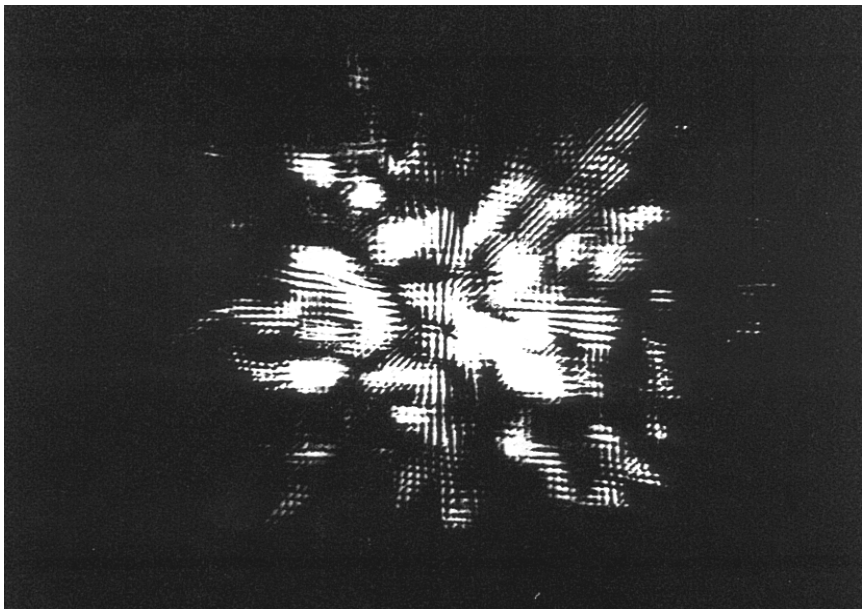

Simulation: focal plane of 3 UTs

coherent coupling without adaptive optics

Interferometre ISI
Infrared Spatial Interferometer)
Berkeley/Mt Wilson

$\lambda = 10.6\ \mu m$

Oscillateur local = laser CO_2

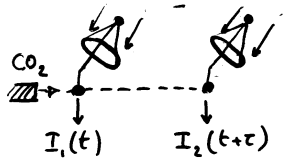

$Re\{ I_1(t)\ I_2^*(t+\tau) \} = S(\tau)$

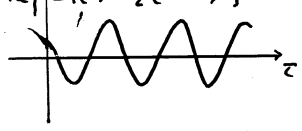

Δt = temps de pose = 270 s

$(1/\Delta t) \simeq 0.004$ Hz .

L'élargissement de la DSP à mi-hauteur est dû à une modulation de fréquence aléatoire de $S(\tau)$: effet d'accordéon .

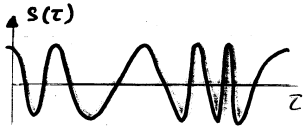

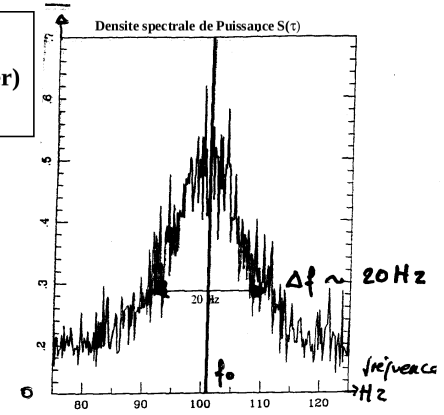

Figure 4-31 Densité spectrale de puissance du signal interférométrique (franges) obtenu par l'interféromètre hétérodyne à 10.6 µm ISI sur l'étoile α Orionis en 1992. La fréquence des franges, proche de 100 Hz, est fixée par la rotation de la Terre, la position de la source dans le ciel et la base *B* (longueur et orientation). Cet enregistrement est particulier car durant cette période d'observation l'atmosphère introduit une phase différentielle importante et variable dans le temps entre les deux trajets optiques, produisant un effet «d'accordéon» ou de modulation de fréquence sur les franges. Celui-ci se traduit par un élargissement significatif (≈ 20 Hz) du pic de densité spectrale et une diminution corrélative de son amplitude. Durée totale d'observation 4.5 minutes. (D'après Townes C. H. *et al., Infrared Physics*, 35, 1994.)

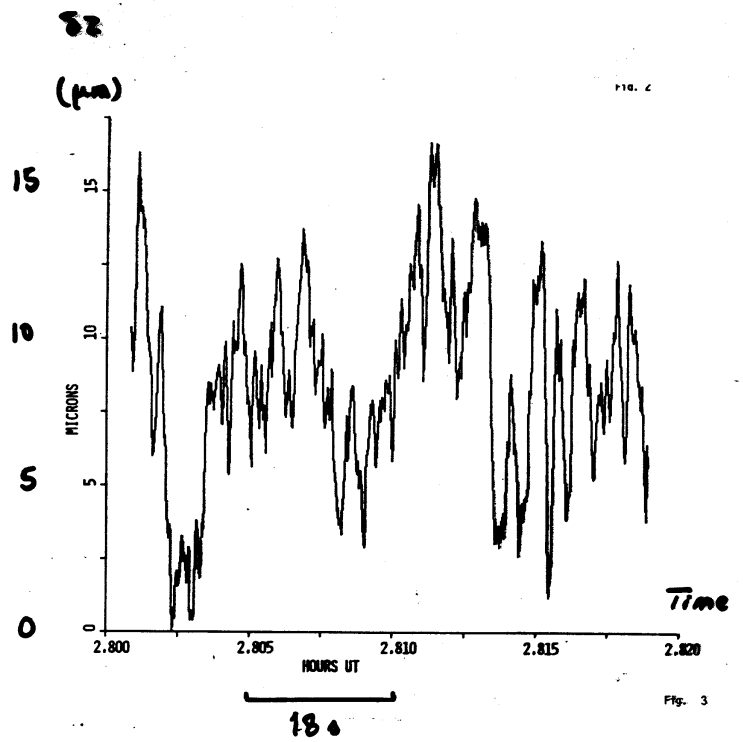

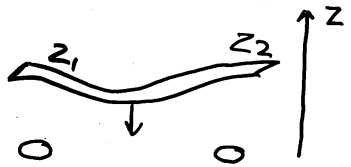

$\delta z = z_1 - z_2$

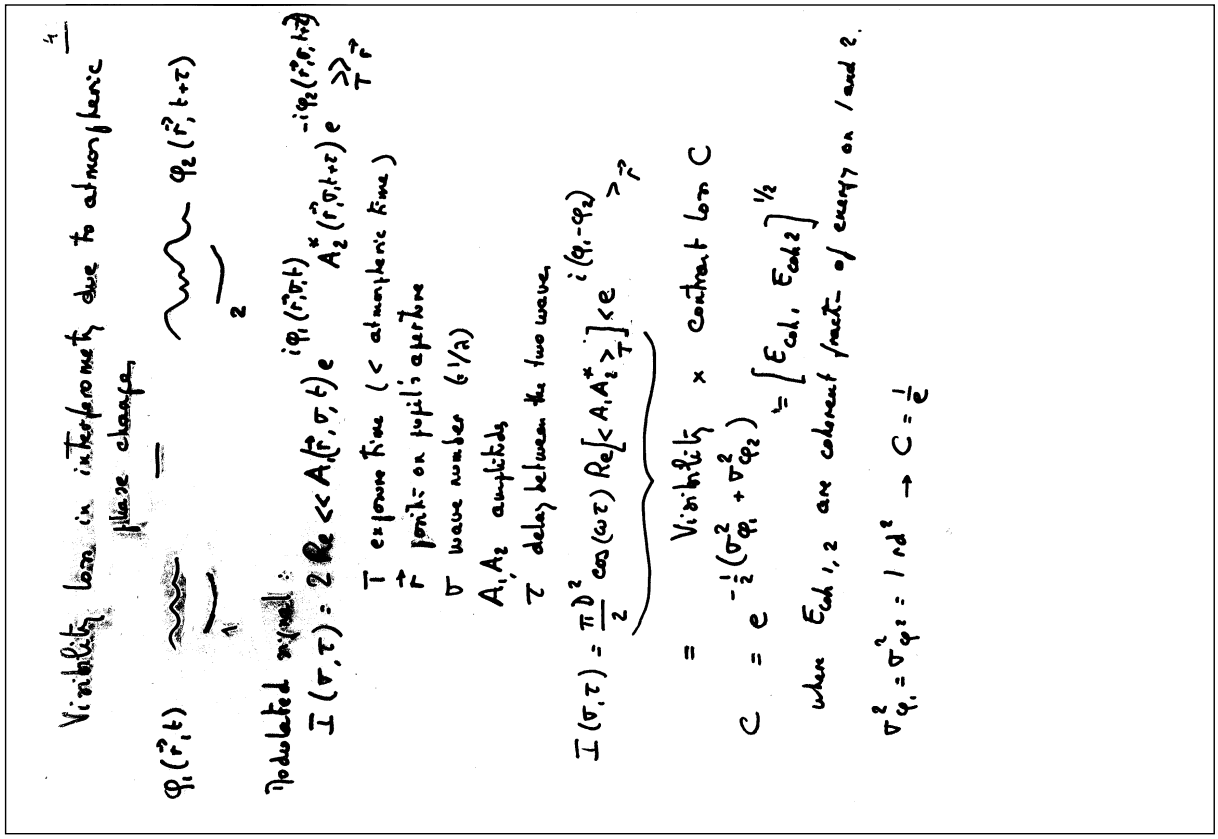

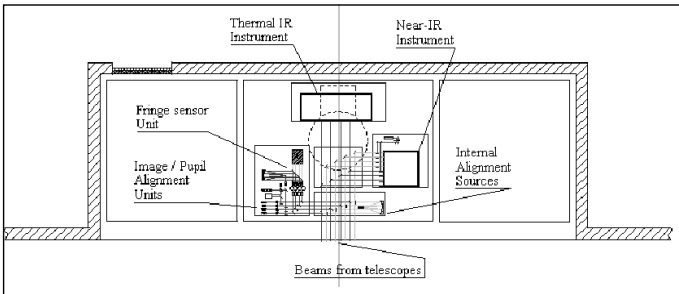

8. Methods of light recombination

- **Internal metrology in an interferometer**
- **Image plane recombination**
  - **dispersed fringes & spectral analysis**
  - **pupil reconfiguration ($N_{\text{télescopes}} > 2$)**
- **Pupil plane recombination**
  - **Double Fourier spectral analysis**
- **Integrated optics recombiners**
- **Dual-beam (dual-feed) operation**

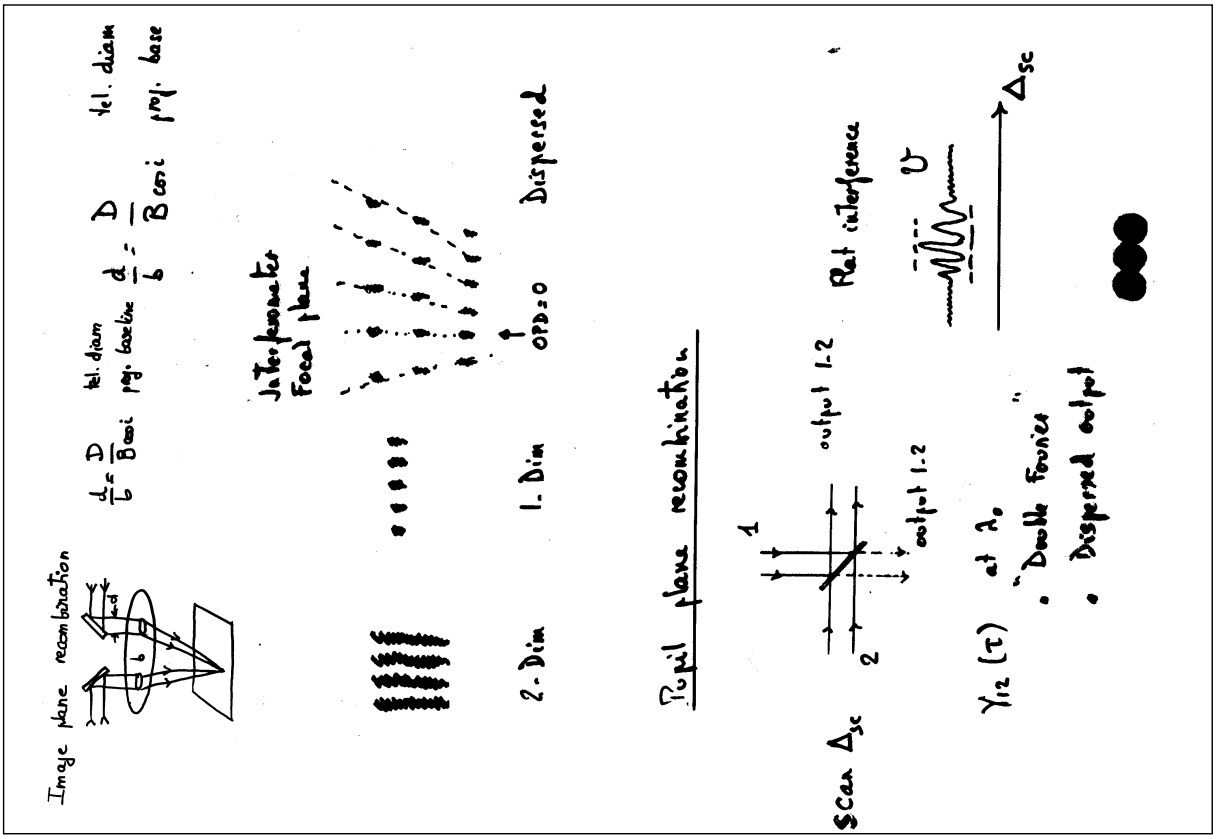
Image plane recombination
tel. diam
proj. baseline
D/B
Interferometer Focal plane
Dispersed
1. Dim
OPD=0
2. Dim
Pupil plane recombination
output 1.2
output 1.2
Scan Δsc
Fast interferences
Δsc
"Double fringes"
Dispersed output
γ12 (τ) at λ0

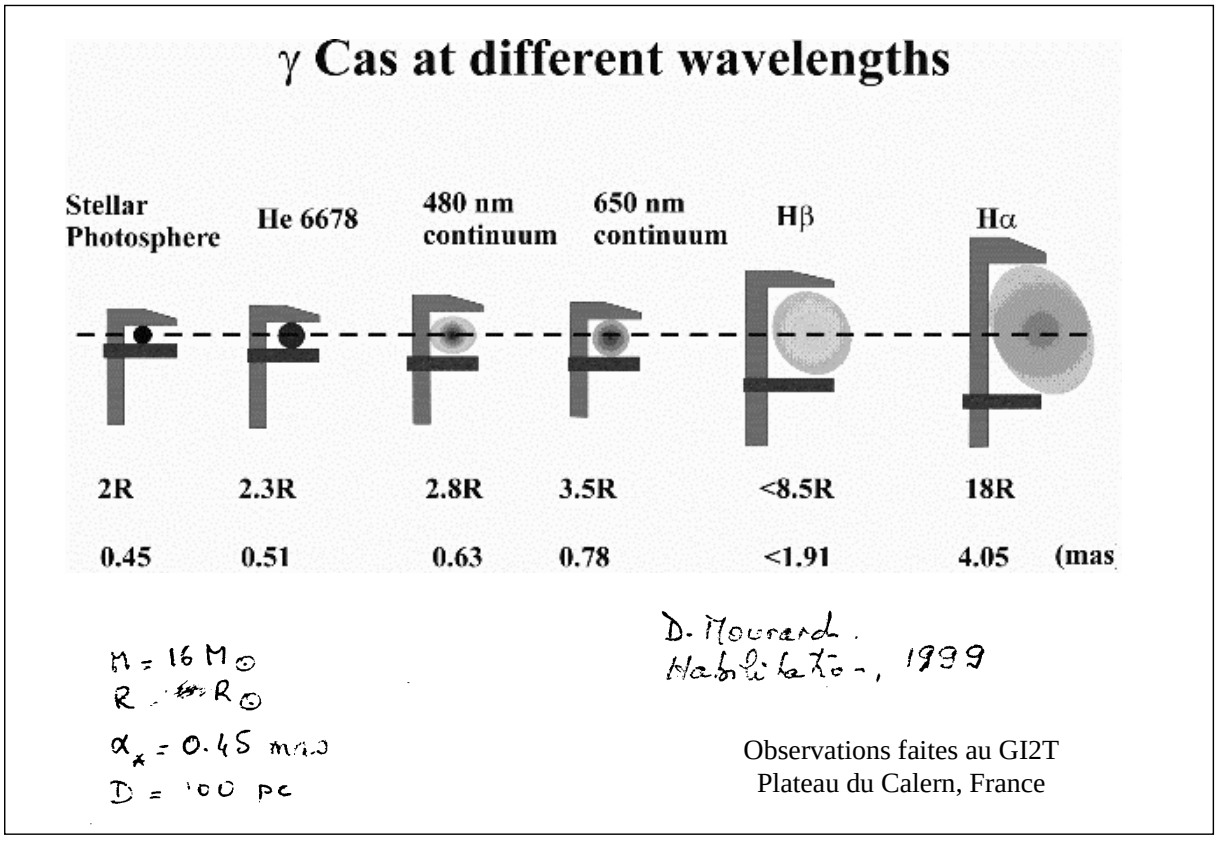
γ Cas at different wavelengths
Stellar Photosphere
He 6678
480 nm continuum
650 nm continuum
Hβ
Hα
2R
2.3R
2.8R
3.5R
<8.5R
18R
0.45
0.51
0.63
0.78
<1.91
4.05
(mas
M = 16 M⊙
R = R⊙
αx = 0.45 mas
D = 100 pc
D. Mourard. Habilitation, 1999
Observations faites au GI2T
Plateau du Calern, France

Angular Diameter of P Cyg in Hα and HeI6678

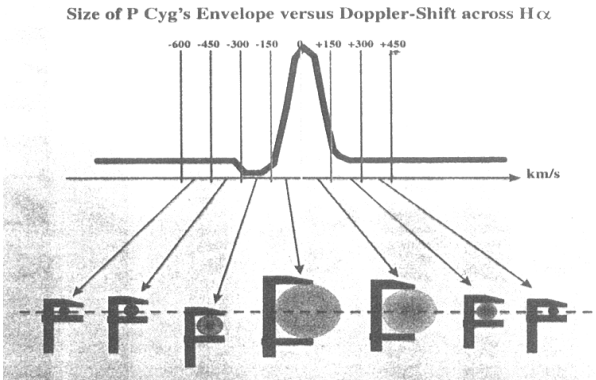

Pictorial Representation of P Cyg as a Function of Doppler-shift Across Hα Emission Line : the Slide Calipper Represents the Interferometric Process to Estimating the Equivalent Uniform Disk Size of P Cygni

Schematic Morphology of P Cyg Wind Projected on the Sky According to GI2T Observations. The Extent of Hα and HeI6678 Envelopes are Given in Units of Photospheric Radius Assumed as 76 ± 15 $R_\odot$ and Corresponding to 0.4 mas. The Angular Scale is Given in mas Taking a Distance of 1.8 ± 0.1 kpc.

The Projected Position of the Detected Blob is at 4 R_* to the South of P Cyg but its Absolute Position in the E-W Direction Remains Unknown.

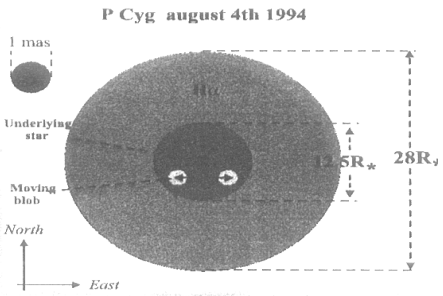

9. Signal detection & noise sources, sensitivity

- From measured to real visibility : calibration
- Expression of the interferometric signal : amplitude & phase
- Noise sources
  - signal photon noise
  - background (thermal) noise
  - detector read-out noise
  - atmospheric noises (piston, scintillation)
- Sensitivity & accuracy
- Phase determination
  - differential
  - phase closure

FRINGES = Visibility x $e^{i\Phi}$

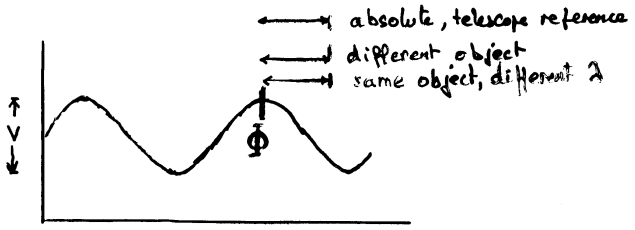

Interferometric sensitivity

Signal = Intensity . Area. Bandwidth. Exposure time. Transm.Visibility.Strehl
Atmosph. piston

Noise = **Signal Photon (visible)**
Read-out (J,H,K)
Background (L,M,N)

Exposure time = **Atmospheric piston stability (ca. 50 ms)**
Long integration if fringe tracking (hours ?)

Transmission = 0.3 to 0.01

Strehl = 0.5-0.7 if proper AO correction ($m_V < 15$)

Visibility = $V_{source} \cdot V_{atm} \cdot V_{mirrors} \cdot \ldots$

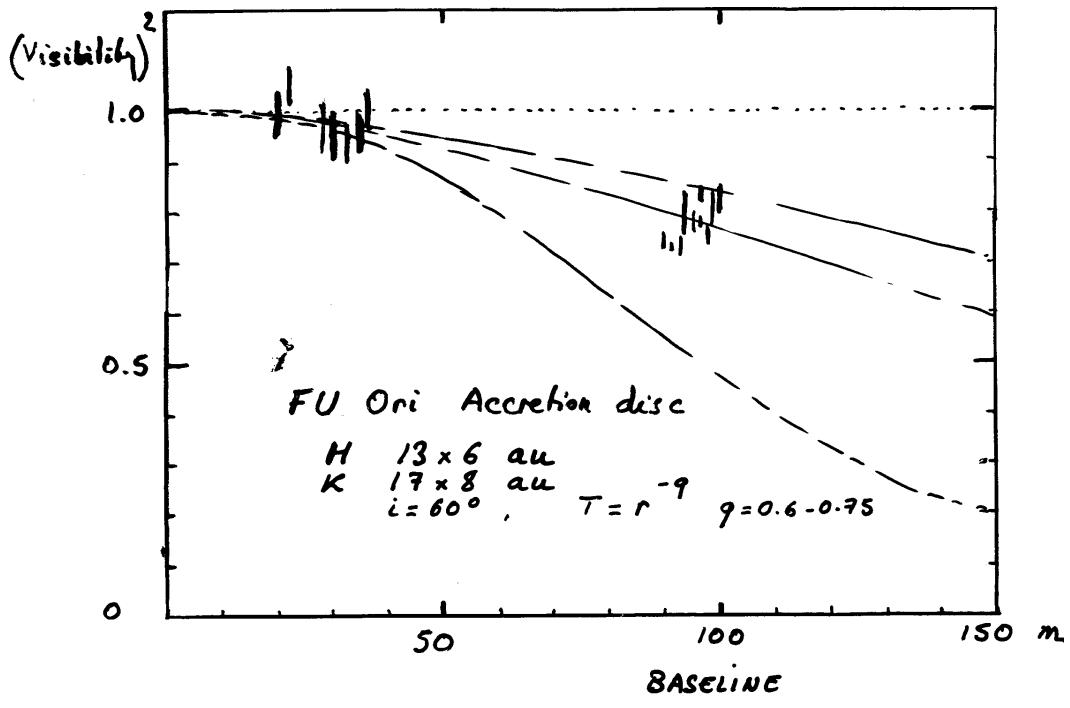

Berger, Malbet, Colavita et al.
SPIE/ESO 2000

PTInterferometer

FLUOR conceptual design

FLUOR Instrument is installed
on IOTA interferometer, on Mt Hopkins

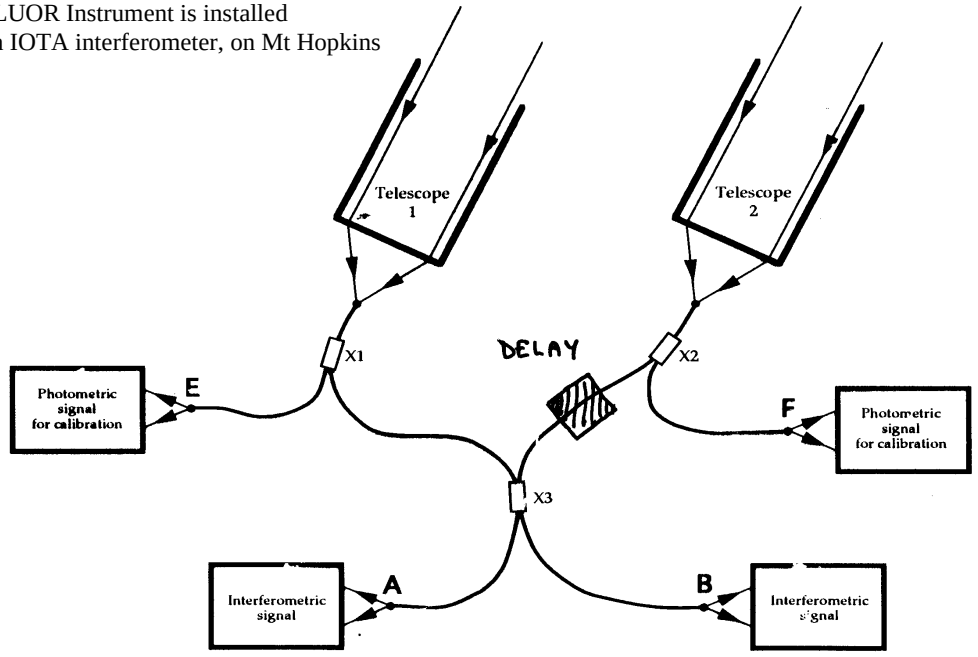

Coude du Forento, Manotti, Ridgway 1993

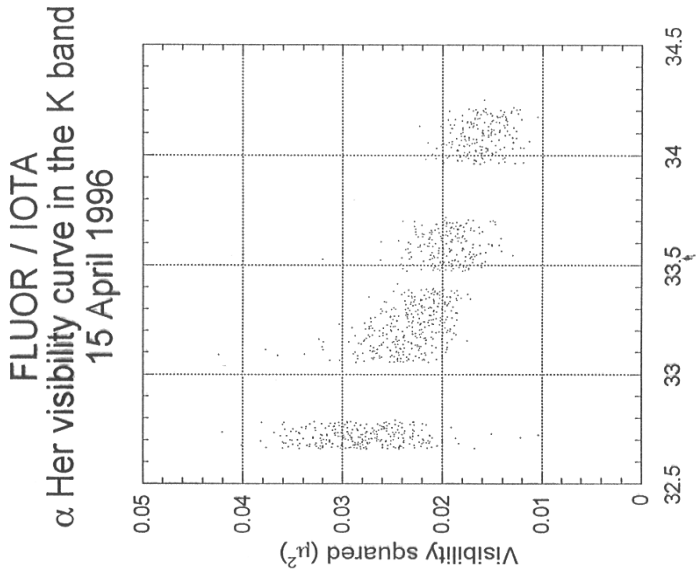

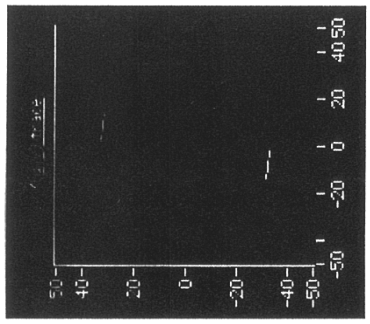

Perrin and Coude du Foresto JMM - 1996

IOTA diam= 45cm
Lmax=38m
Lmin= 5m
L-shaped
Mt Hopkins, Arizona

Performances MIDI (Rapport 1998, Leinert et al, ESO/SPIE 20

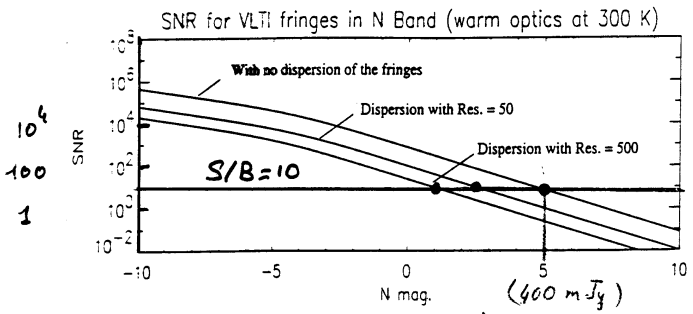

magnitude N

100 msec exposure ("bright" object)

If 10 s exposure (fringe track on reference),
$\Delta m_N \approx 2.5$

NGC 253, 1068, 3758, 5128, Circinus

(12 in complete list above 400 m Jy)

Gain en précision apporté par les fibres

Mesures de visibilités en bande K (2.0 - 2.4μm)

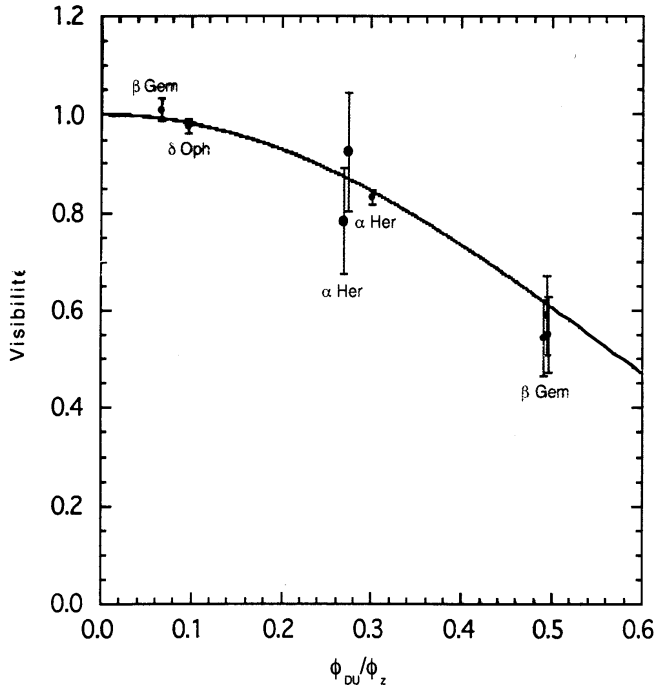

Interféromètres classiques:

IRMA: Benson et al., Astr. J. 105 (1993)
I2T: Di Benedetto and Rabbia, A&A 188 (1987)

Interféromètre à fibres:

FLUOR: Coudé du Foresto, PhD thesis (1994)

AMBER - The J,H,K VLTI instrumen

K limiting magnitudes (conservative)

mode	exp. t.	resol.	K= (UT)	K= (AT)
High precision	0.01 s	5	11.3	8.0
High sensitivity	0.1 s	5	13.2	9.9
Fringe tracking	4 h	5	17	12.1
" "	4 h	100	16.5	11.6
" "	4 h	1,000	15.0	11.1
" "	4 h	10,000	14.2	9.6

Richichi et al., ESO/SPIE 2000

There measurement

2 apertures, 1 source } impossible

2 apertures, 2 sources } Ground : $\delta\theta \lesssim 1$ arc min
Space : $\delta\theta$ arbitrary + internal metrology

≥ 3 apertures, 1 source } Ground : phase closure
Space : internal metrology

Simple case : Photon-noise (signal)

$$\sigma_\varphi = \frac{2}{\pi} \vartheta \sqrt{N} \qquad N \text{ photon / frame}$$

~ 0.1 rd (COAST)

! atmospheric

σ_φ ($\vec{B}$, turbulence, $\delta\theta$)

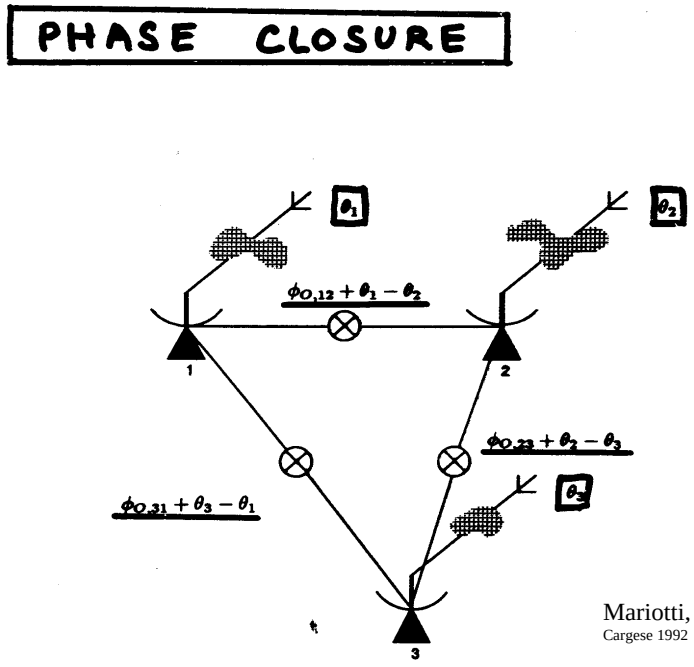

Figure 1. Measured phases for a simple three-element interferometer. $\phi_{O,12}$, $\phi_{O,23}$ and $\phi_{O,31}$ represent the true visibility phases that would be measured in the absence of turbulence. θ_1, θ_2 and θ_3 are phase errors associated with each telescope.

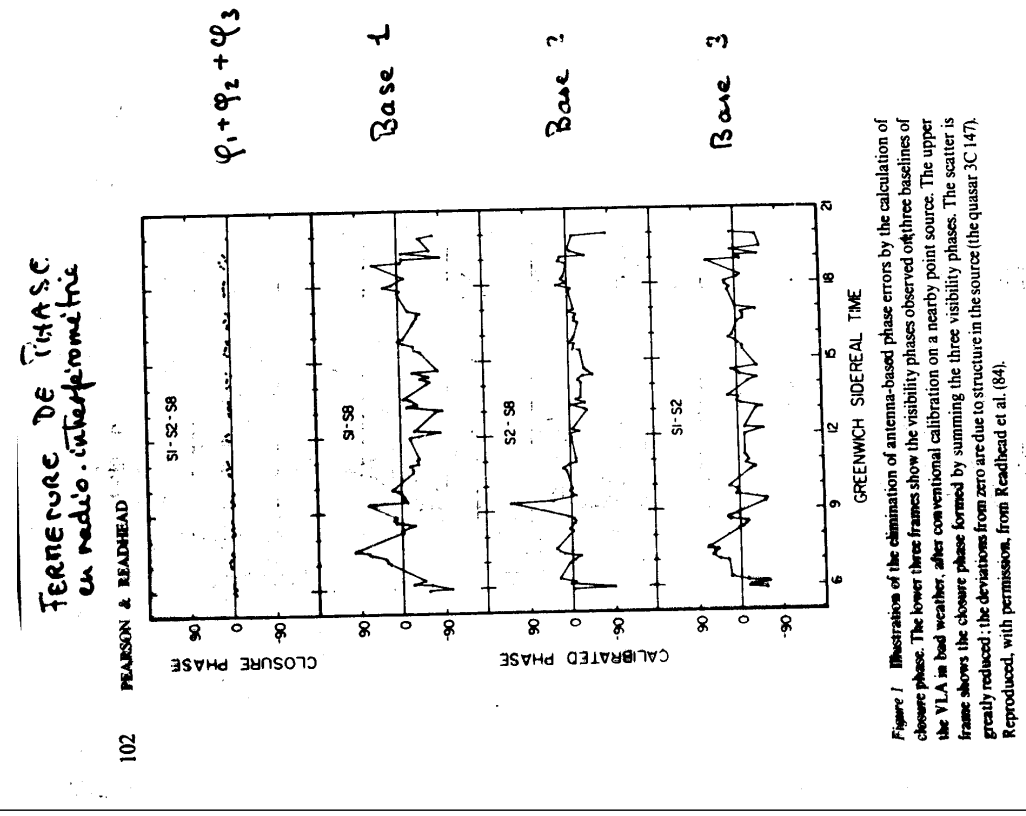

Figure 1 Illustration of the elimination of antenna-based phase errors by the calculation of closure phase. The lower three frames show the visibility phases observed on three baselines of the VLA in bad weather, after conventional calibration on a nearby point source. The upper frame shows the closure phase formed by summing the three visibility phases. The scatter is greatly reduced; the deviations from zero are due to structure in the source (the quasar 3C 147). Reproduced, with permission, from Readhead et al. (84).

SFO - Bordeaux - 1999

Détection directe (3) : annulation interférométrique de l'étoile (*nulling*)

Rapport d'intensité étoile/planète = 10^{-9}-10^{-10} aux λ visible, 10^{-6}-10^{-7} dans l'IR (5-20 μm)

- Bracewell 1979
- Angel 1986, 1997
- Mariotti 1997,1999(+)

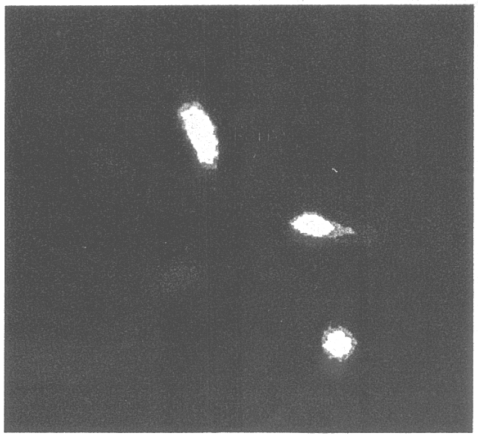

Système solaire à 10 pc, λ = 10 μm
Menesson et al 1998

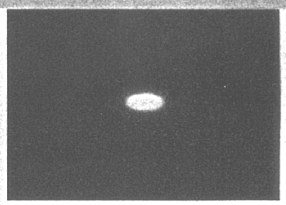

β Pic

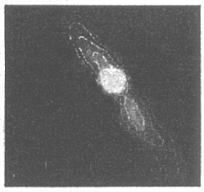

Exo-lumière zodiacale : à λ =10 μm, brillance de la lumière zodiacale du Syst. sol. est 300 x Flux(Terre)

Simulations de *nulling*,

3 planètes telluriques à 10 pc, modulation interne
Menesson 1999

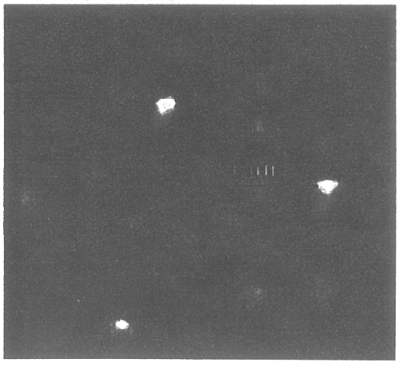

This page was intentionally left blank